ISBN: 978-3-95450-191-5 doi:10.18429/JACoW-SRF2017-MOPB080

THE STABLE OPERATION OF MPG AND MEASUREMENT OF OUTPUT

B. T. Li, D. Y. Yang, L. Xiao, J. F. Zhao, X. Y. Lu†, Y. J. Yang, Z. Q. Yang,
State Key Laboratory of Nuclear Physics and Technology, Beijing , China

Abstract

This paper presents the energy spread measurement result of electron beam produced by MPG. The operation parameters and the experimental result are reported. The average current density of 1.8 mA was obtained at 2.856 GHz. The energy spread of the electron beam is also measured, in which the energy of the most electrons is less than 50 eV and the FHWM is less than 15 eV. The fifth order operation mode is obtained.

INTRODUCTION

The development of electron sources with high current, short pulse, low emittance, good stability has been a challenging topic in the field of accelerators. RF-gun uses microwave electric field to generate electrons, which can provide high quality beam.

The concept of micro-pulse electron gun was put forward in 1969[1]. It was thought to be a very promising electron source with wide range of application. Tsinghua University [2,3], University of Science and Technology of China [4,5], China Academy of Engineering Physics [6], Shanghai Institute of Applied Physics [7] and Peking University have done some research on MPG [8,9]. But after many years of research, it is still not put into practical application because of the unstable operating state and the unknown beam qualities.

In this paper, the design and operation results of a novel MPG are reported. Its stability has been greatly improved. The electron energy spread of the beams was measured by a retarding field energy analyzer.

THEORATICAL ANALYSIS

For MPG with negative feedback mechanism, it is necessary to meet two requirements to guarantee its stable operation: self-bunching requirements and material characteristics. To meet the above requirements, the MPG has to work at a suitable peak cavity voltage, which should be between the characteristic peak cavity voltage and the minimum peak cavity voltage [8,9].

According to the simulation in Ref. [9] and the primary experimental result, the energy of the electrons is about 30eV and the length of the bunch is about 10ps. Based on the conditions above, the energy spread of the beam is measured by a retarding field energy analyzer as shown in Figure1 which utilizes a retarding field to decelerate the electrons.

Assume that the energy spectrum of a given energy E is

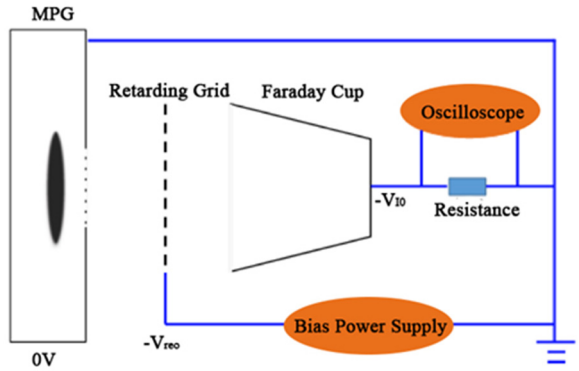

Figure 1: The layout of the energy spread measurement system.

$$S(E_0,T,f,E,k)=\frac{I_s(E)}{I_0} \quad (1)$$

in which E_0 is a specific field intensity of the MPG cavity, T is the transmittance of the grid, f is the frequency, k is the material's secondary electron multiplication parameter, $I_s(E)$ is the beam density composed of electrons that reached the collector overcoming the retarding field, I_0 is the beam density without the retarding field. So the energy spectrum can be expressed as

$$\frac{d\delta}{dE}=\frac{\partial S(E_0,T,f,E,k)}{\partial E} \quad (2)$$

The minus ensures that the result is positive.

$$\frac{d\delta}{dE}=-\frac{1}{I_0}\frac{\partial I_s}{\partial E} \quad (3)$$

SOFTWARE SIMULATION RESULTS

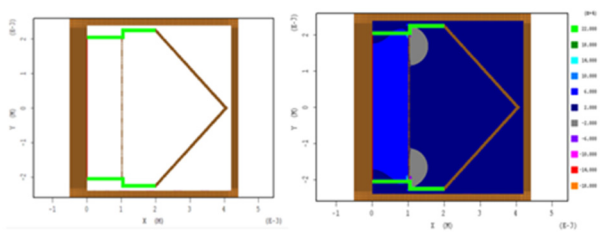

Figure 2: Simulation diagram and X-direction electric field distribution.

We use MAGIC to simulate the electron beam motion during the operation of the retarding field energy analyzer, the simulation results are as shown in Figure 2. The distance between electron emission surface and cathode is 1mm, the simulation time is 3.5ns. The beam size is

† email address: xylu@pku.edu.cn

ISBN: 978-3-95450-191-5 doi:10.18429/JACoW-SRF2017-MOPB080

changed from the original diameter of 4mm to 2mm in diameter and the structure of Faraday cup is also changed in order to save the simulation time. The energy of electrons is 28eV, the length of the Faraday cup is reduced, and the above improvements have no effect on the experimental results since they have the same principal. The average flow intensity during simulation is about 3mA, the length of the bunch is 10ps, the grid size of the deceleration grid is 30μm, the spacing between the grids is 30μm. The yellow part of the figure is metallic material, the green part is insulator material. For the materials, the maximum secondary electron emission coefficient is 2.1, the corresponding primary electron energy is 260eV, the emitted secondary electron energy is 2eV. The electric field distribution shows that the electric field distribution in the X direction of the deceleration field is uniform.

Figure 3 shows the movement of the electron beam in the deceleration field energy analyzer at different deceleration field voltages. The initial electron energy is 28eV. It can be seen from the figure that when the voltage is -27V, the spatial width of the electron beam is gradually compressed into a sheet before it reaches the grid. Some electrons pass through the grid and are collected by the Faraday cup while others hit the grid to excite secondary electrons. When the deceleration voltage is -28V, the length of the transmitted part of the electron beam was significantly elongated. This is because the deceleration field acts on the electrons, the electron energy after the deceleration is lower, and the energy spread is larger and the bunch is modulated longer. The other part of the electrons reaching the grid position can not be bombarded on the grid because the energy and the equivalent voltage of the grid is the same. When the deceleration voltage is -28.2V, the electron beam will be reflected back.

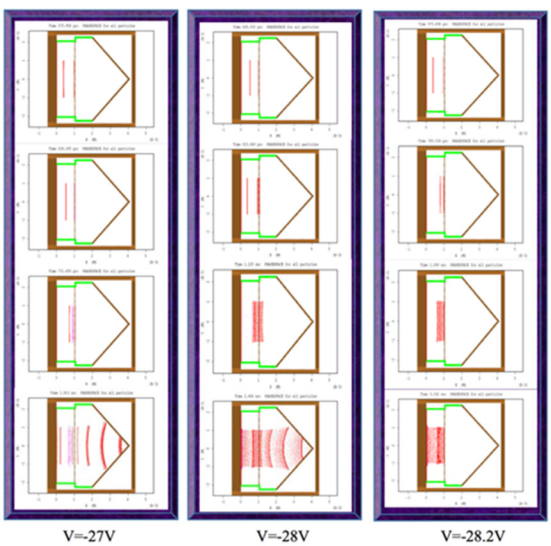

Figure 3: The movement of electron beam in the retarding field energy analyzer under different voltage.

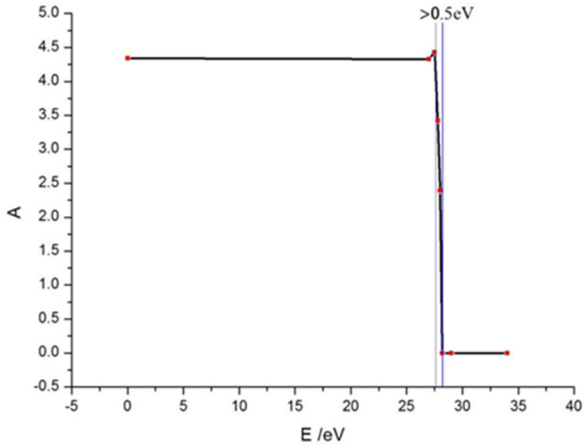

Figure 4: The resolution of the retarding field energy analyzer.

Figure 4 shows the resolution of the deceleration field energy analysis, which is the relative intensity value of the current signal collected by the Faraday cup over a period of time. It can be seen from the graph that the retarding field energy analyzer can analyze the electron beam with energy of 28eV and the energy fraction of the energy analysis is less than 0.5eV, which satisfies the experimental requirement.

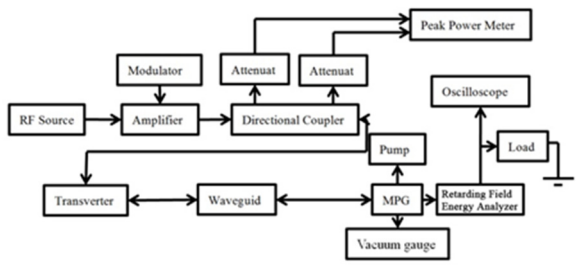

Figure 5: The schematic diagram of the experimental platform.

EXPERIMENTAL SETTLEMENTS

The experimental platform is shown in Fig. 5. The platform is composed of the pump system, the RF power system, the MPG and the retarding field analyzer. The RF power system can provide power up to 1kW. The width of the macro pulse is 10μs to 15μs and the repetition rate is 80Hz to 200Hz which is controlled by the modulator. All the power lines have been calibrated before experiment. The output beam from the MPG cavity is decelerated by the retarding field and then collected by the Faraday cup.

ISBN: 978-3-95450-191-5 doi:10.18429/JACoW-SRF2017-MOPB080

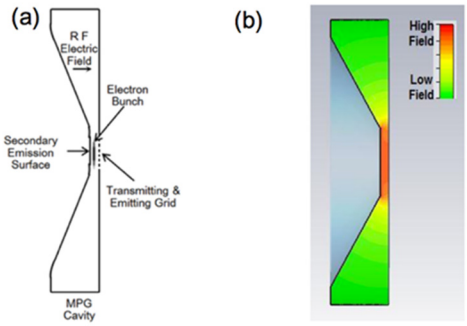

Figure 6: (a)The schematic diagram of the novel S-band MPG model. (b)The RF electric field distribution in MPG.

The MPG is the key part of the platform. The traditional MPG is composed of three parts: an RF pillbox cavity working in the TM010 mode, an emission surface and a grid. The grid allows part of the beam to pass through but is opaque to the input RF field. Basing on this original design, an S-band MPG is proposed as shown in Fig. 6. This kind of MPG shortens the distance between the grid and the emission surface.

As the frequency of the cavity is 2.856GHz, it is determined that the time of movement of electrons from one end to the other is 175ps. According to the above data, the distance of the movement is 1.5mm and it can be adjusted.

A key to keep the MPG running steadily is the treatment of the cathode and the grid. The correct chemical treatment is helpful to get a clean surface and remove surface ripple. Therefore, the cathode and the grid need to be treated carefully before the experiment (Fig. 7). After the cathode was welded to the sample holder, the cathode and the grid were electro polished, using solution mixed with 3:2 ration of n-butanol (99%) and phosphoric acid (85%). Secondly, the cathode was passivated with amino sulfonic acid solution diluted with deionized water. Then the assembled cavity was dehydrated with alcohol and dried with nitrogen. The passivation treatment is helpful to a stable and dense oxide film on the surface. The oxide film allowed the cathode to emit secondary electrons continuously and steadily. Then alcohol was used to dehydrate and nitrogen was used to dry the cathode and grid.

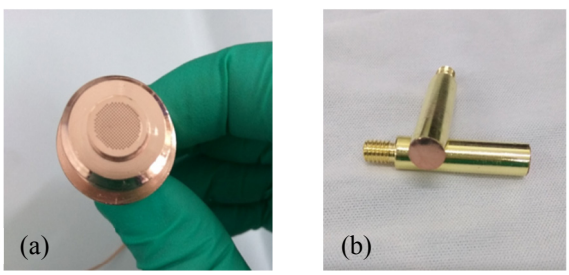

Figure 7: The grid(a) and cathode(b) used in the experiment.

Another key part of the platform is the retarding field energy analyzer, which we used to measure the energy spectrum of the beam. The profile of the retarding field energy analyzer is shown in Fig. 8 and the physical map is shown in Fig. 9. The aperture of the MPG grid is 4mm. The grid on retarding field energy analyzer is laser-etched and made of oxygen-free copper. Its diameter is 10 mm, the transmittance is 40%, the thickness is 20 μm. The distance between the MPG grid and the deceleration grid is 1 mm. The grid is insulated with a PEEK material, connected to a bias power supply via a bias line. Behind the grid is the Faraday cup, a hole is opened on its side through which the MPG can be vacuumed.

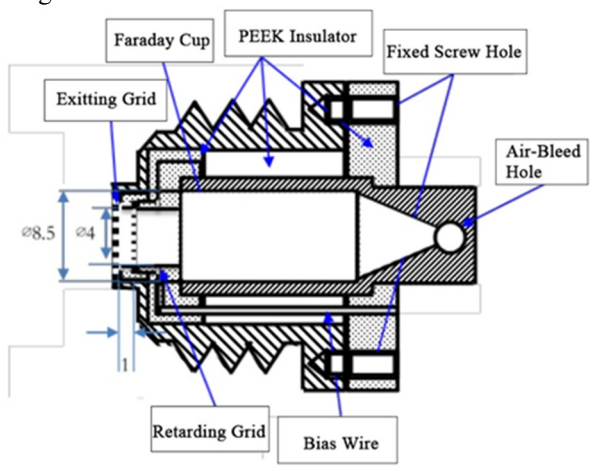

Figure 8: The profile of the retarding field energy analyzer.

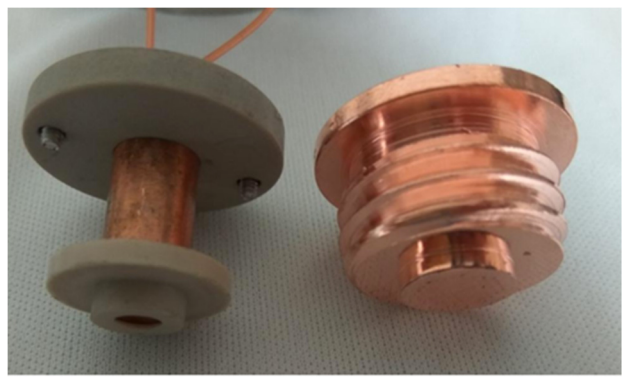

Figure 9: The physical map of the retarding field energy analyzer.

EXPERIMENTAL RESULTS AND DISCUSSION

The treated cathode and grid were loaded into MPG, and the experiment was carried out.

The transmittance of the grid is chosen as 15.5%. The frequency is adjusted to 2.856GHz, the repetition frequency of the macro pulse is 100.1 Hz, the width of the macro pulse is 10μs, the vacuum degree is 5.1×10^{-5}Pa, the forward power is 56.937dBm, the reflection power is 53.687dBm, the distance between the grid and the cathode is adjusted to 1.944 mm, the grounding resistance is 1kΩ. In order to accelerate the air bleeding process on the surface, the cavity was baked at 60 °C for 56 hours. The obtained current signal waveform is shown in Fig. 10.

ISBN: 978-3-95450-191-5 doi:10.18429/JACoW-SRF2017-MOPB080

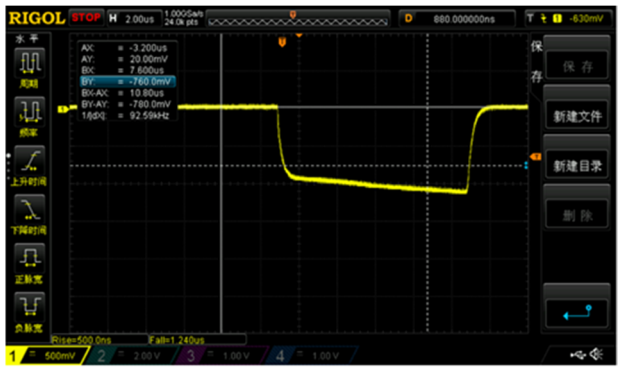

Figure 10: The flow intensity signal obtained by oxygen-free copper grid and cathode.

Figure 11 shows the flow signal at different times during the experiment. The attenuation coefficient of the probe is 0.36. It can be seen from the figure that during the first 10 hours, the beam flow is quite stable. After 11 hours of operation, the output of the pulse is divided into two levels, the general pulse amplitude is small, while occasionally the output can reach the same amplitude as the strong pulse during stable operation. After 50 hours of continuous output, the output of the micro-pulse electron gun has become extremely unstable, with only a few macro pulses having a beam output.

After calculation, the average flow intensity at the beginning is 1.8mA and the variance is 0.037mA. After 10 hours, the average flow intensity of the beam is 1.69mA, the variance is 0.053mA.

The current of the electron beam passed through the retarding field was measured by the Faraday cylinder. The current intensity (Fig. 12) represents the number of electrons collected by the Faraday cylinder, which also means the number of electrons with the corresponding energy.

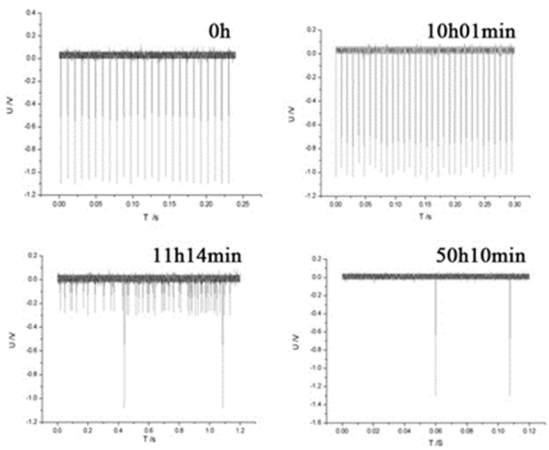

Figure 11: The flow signal at different times during the experiment.

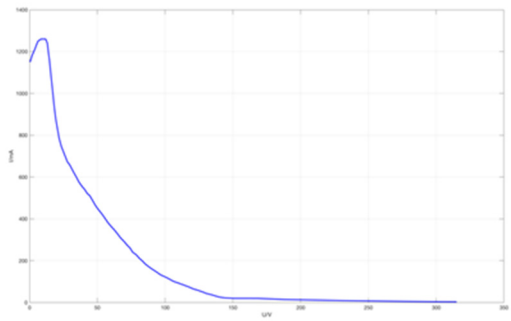

Figure 12: Experiment result of the output current.

The result of energy spread which is obtained by differentiating the output current respected to the retarding voltage is shown in Fig. 13.

It is worth noting that when the energy is less than 10eV, there is a negative value in the spectrum, which shows that the flow intensity collected by Faraday cup is gradually increasing as the retarding field energy increases. This is because the retarding voltage is small in this interval, the electron beam generated from the MPG goes through the retarding grid and hits the Faraday Cup to excite secondary electrons. The energy of the secondary electrons excited by electrons with energy between 30eV~300eV is below 10eV,[10] part of the excited secondary electrons will hit the retarding grid. Since their energy is below 10 eV, they cannot effectively excite secondary electrons and this part of the electrons will be collected by the grid. In view of the above, the number of net electrons collected by the Faraday cup will gradually increase as the retarding voltage increases between 0 and -10V. Most electrons' energy is lower than 50eV. The energy spread is about 15eV. This suggests that when the secondary electron emission coefficient is about 1, the energy of the electrons emitted by MPG is lower than 50eV, which is consistent with the data proposed by Furman [10] and Hilleret [11] of Lawrence Berkeley National Laboratory.

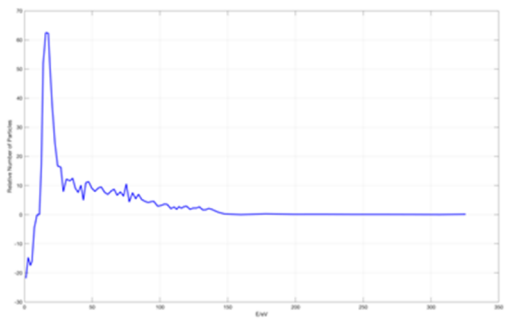

Figure 13: Experiment result of the energy spectrum.

Since the energy of electrons is about 35eV, they cannot reach another multiplier in half a cycle. Assuming that the emission energy of the electrons is 2eV and the energy reaching another multiplier is 35eV, the corresponding velocities are $8.4 \times 10^5 \mathrm{m/s}$ and $3.6 \times 10^6 \mathrm{m/s}$ respectively. If the fifth-order model is adopted, the transit time is 875ps, then the travel distance is 1.94mm, which is

ISBN: 978-3-95450-191-5 doi:10.18429/JACoW-SRF2017-MOPB080

consistent with the experiment settlement. So it can be inferred that the electrons in the cavity are mainly operating in the fifth order mode.

The main source of error is the lens effect at the grid [12]. As electron optical texts show, there is a lens existing between two fields [13]. In the case of a parallel plate retarding field energy analyzer , the focal power is

$$\frac{1}{f} = -\frac{1}{4d} \tag{4}$$

d is the distance between the exiting grid and the retarding grid. The negative sign signifies a divergent action. Hence after passing through a hole on the grid, a beam will have a divergence

$$\theta \approx sin\theta = \frac{r_0}{f} = \frac{r_0}{4d} \tag{5}$$

r_0 is the entrance aperture. And the energy resolution can be expressed as

$$\frac{\Delta E}{E} = \frac{r_0^2}{16d^2} \tag{6}$$

There are several possible reasons for the decline of the stability of MPG. Firstly, the state breakage of the cathode and the grid of the cavity, which may destroy the electric field structure of the cavity or produce undesired plasma. Secondly, the charge accumulation effect of the insulator in the test system may also be another inducement factor. The incidental field distortion may change the track of the electrons so that the electrons couldn't be collected by the Faraday cylinder.

CONCLUSION

This paper presents an experimental result of the energy spread of the MPG beam. The energy spread measurement system was established based on a high-accuracy retarding field analyzer. The experiment results show that the secondary electrons can be produced with energy lower than 50eV and the spread of the energy is about 15eV. The MPG operated steadily for more than ten hours and the fifth order operation mode is observed.

ACKNOWLEDGEMENTS

This work was funded by State Key Laboratory of Nuclear Physics and Technology.

REFERENCES

[1] W. J. Gallagher, "The multipactor electron gun", in Proceedings of the IEEE, vol. 57(1), pp. 94–95, 1969.

[2] J. Y. Zhai *et al.*, "Experimental study on the beam dynamics of the micro-pulse electron gun", *High Energy Physics & Nuclear Physics*, vol. 30(2), pp. 99–101, 2002.

[3] J. Y. Zhai *et al.*, "Multipactor electron gun with cvd diamond cathodes", in *Proc. EPAC* 2006, paper THPCH174, pp.3203-3205.

[4] W. C. He *et al.*, "Simulation and analysis of secondary emission microwave electron gun", *High Power Laser & Particle Beams*, vol. 13(5), pp. 615–618, 2001.

[5] H. B. Sun, Y. J. Pei, A. G. Xie, R. Wang, "Numerical algorithm of secondary emission microwave electron gun", *High Energy Physics & Nuclear Physics*, vol. 29(1), pp. 95–98, 2005.

[6] X. F. Yang *et al.*, "Analysis and experimental design of micro-pulse gun", *China Nuclear Science & Technology Report*, 2002.

[7] L. Liao *et al.*, "Multipacting analysis in micro-pulse electron gun", *Chinese Physics C*, vol. 37(11), pp. 84–87, 2013.

[8] K. Zhou *et al.*, "Study on the steady operating state of a micro-pulse electron *gun*", *Review of Scientific Instruments*, vol. 85(9), pp. 1172–1180, 2014.

[9] J. Zhao *et al.*, "Theoretical *analysis* and simulation of the influence of self-bunching effects and longitudinal space charge effects on the propagation of keV electron bunch produced by a novel s-band micro-pulse electron gun", *Aip Advances*, vol. 6(6), pp. 411, 2016.

[10] M. A. Furman *et al.*, "Probabilistic model for the simulation of secondary electron emission", *Phys.rev.st Accel. beams*, vol. 5(12), pp. 317–322, 2002.

[11] I. Bojko *et al.*, "Influence of air exposures and thermal treatments on the secondary electron yield of copper", *Journal of Vacuum* Science *& Technology A Vacuum Surfaces & Films*, vol. 18(3), pp. 159–167, 2000.

[12] J. A. Simpson, "Design of retarding field energy analyzers", *Review of Scientific Instruments*, vol. 32(12), pp. 1283–1293, 1961.

[13] V. K. Zworykin *et al.*, *Electron optics and the electron microscope*, John Wiley & sons, inc, 1957.